

Scaling properties in the packing of crumpled wires

C. C. Donato, M. A. F. Gomes, and R. E. de Souza

Departamento de Física, Universidade Federal de Pernambuco, 50670-901, Recife, PE, Brazil

(Received 22 September 2002; published 13 February 2003)

Statistical properties of configurations of a metallic wire injected into a transparent planar two-dimensional cavity for three different injection geometries are investigated with the aid of high-resolution digital imaging techniques. The observed patterns of folds are studied as a function of the packing fraction of the wire within the cavity. In particular, we have examined the dependence of the mass of wire within a circle of radius R , as well as the dependence of the number of contacts wire-wire with the packing fraction. The distribution function $n(s)$ of connected loops with internal area s formed as a consequence of the folded structure of the wire, and the average coordination number for these loops are also examined. Several scaling laws connecting variables of physical interest are obtained and discussed and a relation of this problem with disordered two-dimensional foam and random packing of disks is examined.

DOI: 10.1103/PhysRevE.67.026110

PACS number(s): 05.70.Np, 05.90.+m, 47.53.+n, 68.35.Rh

I. INTRODUCTION

Dense disordered packing of identical spheres is of basic importance to many branches of industry and science, and theoretical, experimental, and technological investigations of this problem have traditionally attracted much attention over the centuries [1]. Packing of rigid spheres is important in the microscopic theory of fluids, glasses, and crystals [2], as well as in determining the macroscopic granular structure of powders and other porous materials. This type of packing is currently studied in physics and mathematics from the point of view of computer simulations [3], simple and innovative experiments [4], and sophisticated theoretical tools [5]. Three-dimensional (3D) packings of nonspherical objects, such as ensembles of spheroids [6], rods [7], cuboids [8], crumpled wires and crumpled surfaces [9], among others, have also been studied with many types of algorithms. Higher-dimensional versions of dense packings of spheres are of current interest in dual theory and superstring theory, as well as in problems arising in digital communications [5].

Two-dimensional packing of hard discs has been comparatively much less studied, despite its intrinsic theoretical interest and its importance in the structure of monomolecular films [2] and its connection with several different packing problems in geometry [10]. A number of other 2D packing problems involving random mixtures of discs [11], squares [12], and regular polygons [13] have also been discussed in the literature.

On the other hand, in spite of the great scientific and technological importance of phenomena associated with crumpled structures of microscopic and macroscopic materials, our understanding of the geometric and physical behavior of these systems is still limited. In the last years, theoretical and experimental aspects of the condensed matter physics of crumpled sheets have been a subject of growing interest in many areas of study, e.g., acoustic emission [14], continuous mechanics [15], growth models [16], packing problems [9], polymer, membrane, and interface physics [17], universality [18], among others. Crumpled structures with different topologies, as exemplified by a squeezed ball of wire, have been much less studied in the physics litera-

ture. The geometrical, statistical, and physical aspects of crumpled wires in 3D space were examined ten years ago from the point of view of experimental work and analogic simulations, and in particular some robust scaling laws and fractal dimensions associated with these disordered systems were observed [19]. The geometric aspects observed in the packing of crumpled wires may be relevant to biological applications, as for example, in the study of DNA compaction in the chromosomes, as well as in the study of supercoiled DNA structures in the processes of replication and recombination [20,21].

In the present paper, we report the results of an extensive experimental analysis of the packing of 2D crumpled structures obtained by irreversible squeezing of macroscopic pieces of copper wires within a *two-dimensional* transparent cavity. Irreversibility here means that if the constraints due to the cavity are removed, the crumpled wire does not restore the initial configuration. In this work we use high-resolution digital images to study quantitatively some important aspects of the statistical physics of the packing structure of 2D crumpled wires. These structures are *remarkably* different from crumpling processes of sheets in 3D. Some of our conclusions (mostly related to a single injection geometry) have been summarized elsewhere [22]. Here we give a more detailed exposition, and present some results. In particular, a comparison is made between the packing process of crumpled wires and the classical problems of the random packing of disks and disordered 2D foam.

The outline of the article is as follows. In Sec. II we describe the experimental details of the problem, and in Sec. III we present our experimental results and a discussion of our main findings. Section IV is devoted to a discussion concerning some similarities observed in the geometric and mechanical properties of crumpled wires, packing of disks, and disordered 2D foam. In Sec. V we summarize our major conclusions.

II. EXPERIMENTAL DETAILS

The experimental apparatus used in our work to register 2D configurations of crumpled wires is shown in Fig. 1. It

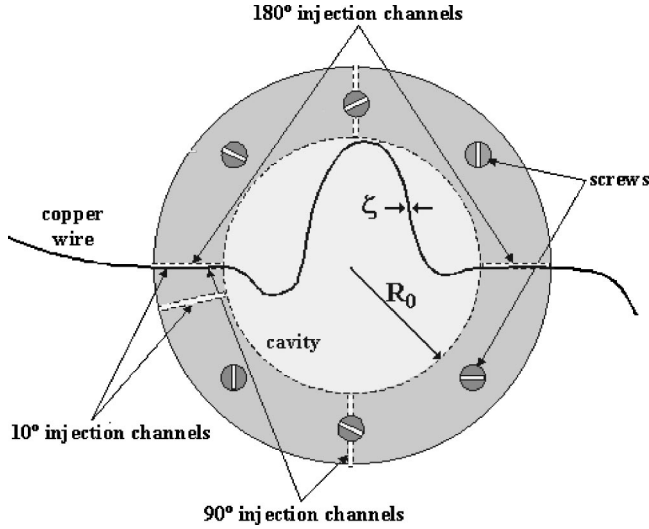


FIG. 1. Diagram of the 2D injection cell used in the experiments discussed in this paper. See Sec. II for details.

consists of a transparent cell formed by the superposition of two disks of Plexiglass with a total height of 1.8 cm, an external radius of 15 cm and a circular cavity with radius $R_0 = 10$ cm and 0.11 cm of height, which can accommodate configurations of a *single* layer of crumpled wire. The cavity of the cell was polished and the copper wire used in the experiments (#19AWG) had a diameter $\zeta = 0.10$ cm and a varnished surface, in order to reduce the friction. Cavity and wire operated in dry regime, free of any lubricant. Four radial channels were made to provide three different ways of injection of wire into the cell at the angles $\theta = 10^\circ$, 90° , and 180° , as suggested in Fig. 1. The photographs were taken with an Olympus C-3040ZOOM digital camera with resolution of 2048×1536 pixels, which was assembled 30 cm over the cell. To avoid picture artifacts by light reflections a cylindrical paper screen was placed around the cell as well as lighting was carefully controlled. Afterwards the digital images were transferred to a personal computer where images were digitally processed. This stage, in general, consists of five steps. In step 1, lighting corrections are performed. This is quite worth because the light reflections on the varnished surface of the wire become the boundary wire image somewhat undefined. In step 2, the circular area corresponding to the cavity is removed. In step 3, the length of the wire is computed by counting imaging pixels and the result is compared to the length of wire, previously measured. We have accepted a image as valid data when the percent relative error is less than or equal to 3%. In step 4, we have converted the original RGB image standard into binary image. The cavity background and wire become white and black, respectively. In step 5, all subsequent specific processing to compute mass-size relation, box counting for 2D, number of loops, perimeter of loops, etc., are implemented. At this point, it is interesting to discuss briefly some basic and qualitative aspects of the 2D crumpled structures studied in this paper. First, when a thin flexible wire of length L is injected inside a cavity of the type shown in Fig. 1, the wire bends if its length is slightly larger than the diameter of the cavity,

$2R_0$. Second, as more wire is injected, there is a critical length $L = h_1$ when the wire touches itself forming the first loop. If we define the ratio $\eta = h_1/2\pi R_0$ we then obtain $\eta = 0.68 \pm 0.01$; 0.90 ± 0.01 ; and 1.13 ± 0.02 , for $\theta = 180^\circ$, 90° , and 10° , respectively. These numerical estimates for η come from averages on 20 experiments whose intent was to determine the critical length h_1 . An additional indicator of the statistical fluctuations of η is given by the minimum (maximum) values obtained along the 20 measurements of this quantity: η_{min} (η_{max}) assume, respectively, the values 0.67 (0.70), for $\theta = 180^\circ$, 0.89 (0.90), for $\theta = 90^\circ$, and 1.1 (1.15), for $\theta = 10^\circ$. Alternately, the first-contact problem introduced in this paragraph can be specified by giving the corresponding packing-fraction p defined as

$$p \equiv (\text{projected area of the crumpled wire/area of the cavity}) \\ = \zeta L / \pi R_0^2. \quad (1)$$

For the first contact, $p \rightarrow p_{fc} \equiv \zeta h_1 / \pi R_0^2 = 2\eta\zeta/R_0 = 0.014 \pm 0.001$, 0.018 ± 0.001 , and 0.023 ± 0.001 , for injection at 180° , 90° , and 10° , respectively.

For increasing p (or L), the wire begins to crumple progressively into a highly contorted shape as we will show next. In order, for the reader, to develop some insight about the nature of the crumpling process that is considered here, we show in Fig. 2 typical 2D configurations for some different values of the packing fraction p [length L (cm)] = 0.016 [50] [(a), (e), (i)]; 0.048 [150] [(b), (f), (j)]; 0.095 [300] [(c), (g), (k)]; and $p_{max}(\theta)[L_{max}(\theta)(\text{cm})] = 0.150$ [470], for $\theta = 180^\circ$ (d); 0.125 [394], for $\theta = 90^\circ$ (h); and 0.130 [409], for $\theta = 10^\circ$ (l). Figures 2(a), 2(e), and 2(i) indicate the early stages of the crumpling process as we inject the wire into the 2D cavity. Irrespective of the geometry, the experiments begin fitting a straight wire in the corresponding channels associated with a particular geometry and subsequently pushing manually and uniformly the wire on both sides of the cell toward the interior of the cavity. The patterns of crumpled wire observed within the cavity are basically due to the formation of a cascade of loops of decreasing size. During the progressive injection of wire into the cavity, the cascade of loops evolves in such a way that it is common to observe localized or large (global) rearrangements of the loops previously formed, particularly for the case $\theta = 180^\circ$. For $\theta = 10^\circ$ and 90° , the global rearrangements are much more rare. The reader can also observe that the sharp creases and ridges found in crumpling of sheets are absent in the 2D crumpled wires shown in Fig. 2. Figures 2(i)–2(l) show a typical sequence of injection at 10° . The sequence starts forming a circlelike configuration that collapses into a double wire structure that contains loops. This new structure evolves almost as if it were one single cascade of loops, until the size of loops approach the distance between injection points in the cell, which is ≈ 1.7 cm. At this point, the pattern splits up onto two small cascades. The dynamics of crumpling for 90° injection shown in Fig. 2(h) is quite similar to that shown in Fig. 2(l) in the sense that two isolated cascades of small loops are localized near the injection points. The initial injection velocity of wire at each channel

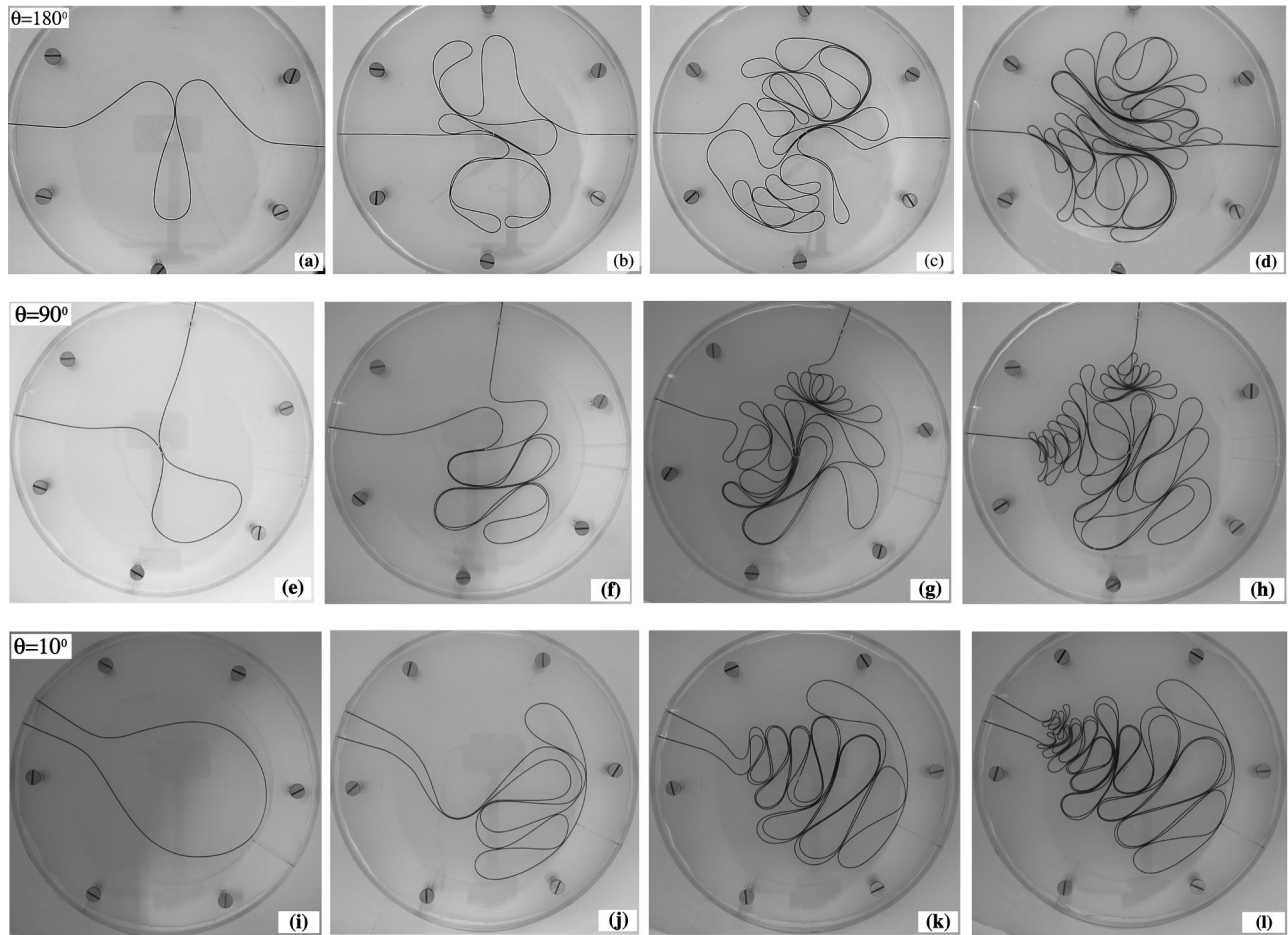


FIG. 2. Typical 2D configurations of crumpled wire for some different values of the packing fraction p [length $L(\text{cm})$] = 0.016 [50] [(a),(e),(i)]; 0.048 [150] [(b),(f),(j)]; 0.095 [300] [(c),(g),(k)]; and $p_{max,\theta}[L_{max,\theta}(\text{cm})]$ = 0.150 [470], for $\theta = 180^\circ$ (d); 0.125 [394], for $\theta = 90^\circ$ (h); and 0.130 [409], for $\theta = 10^\circ$ (l). See Sec. II and III for details.

in the experiments was of the order of 1 cm s^{-1} . However, the observed phenomena are widely independent of the injection speed for all interval of injection velocity compatible with a manual process. When the length of wire within the cavity increases ($p \gtrsim 0.10$), the difficulty of injecting more wire rises, with a corresponding reduction in the velocity of injection. For p near p_{max} , the difficulty in the injection rises abruptly and the crumpled structures finally become rigid: the crumpled wire becomes completely jammed within the cavity and it is practically impossible to continue with the injection of wire for $p > p_{max}$. Thus, the mechanical behavior of the samples is quite different whether we are near or well below p_{max} . The particular moment when the injection velocity goes rapidly to zero leads to a *tight-packing* (TP) configuration for the crumpled wire, as shown in Figs. 2(d), 2(h), and 2(l). Experimental estimates of the maximum *average* (over seven equivalent experiments for each geometry of injection) packing fraction for the three different geometries studied give $p_{max} = 0.14 \pm 0.01$, 0.11 ± 0.02 , and 0.14 ± 0.02 , for 180° , 90° , and 10° , respectively. Our overall estimate points to $p_{max} = 0.14 \pm 0.02$, irrespective of the geometry of injection. To rule out any possibility of the TP configurations being a consequence of friction effects, we carried out experiments where the cavity was filled with min-

eral oil. The results in this case perfectly agree with the dry-regime ones: $p_{max} = 0.14 \pm 0.02$, irrespective of geometry. We can observe from Fig. 2 that the differences in the geometric patterns of crumpled wires for different injection angles are more evident for $p \leq 0.05$ ($L \leq 150 \text{ cm}$). When p increases, these differences attenuate, although the particular symmetry signatures associated to the three geometries of injection studied remain evident. It is important to notice, however, that the critical exponents obtained in the following sections are *independent* (within typical statistical fluctuations of 5–10%) on the particular type of injection symmetry considered. A detailed quantitative study of the configurations of 2D crumpled wires is made in the following section.

III. RESULTS AND DISCUSSION

A. Mass-size relation

One of the most basic physical properties when dealing with growth models, polymer configurations, and fractal structures presenting some degree of statistical isotropy is the dependence $M(R)$ of the mass of the system within a circle of radius R . This quantity is shown in the log-log plots

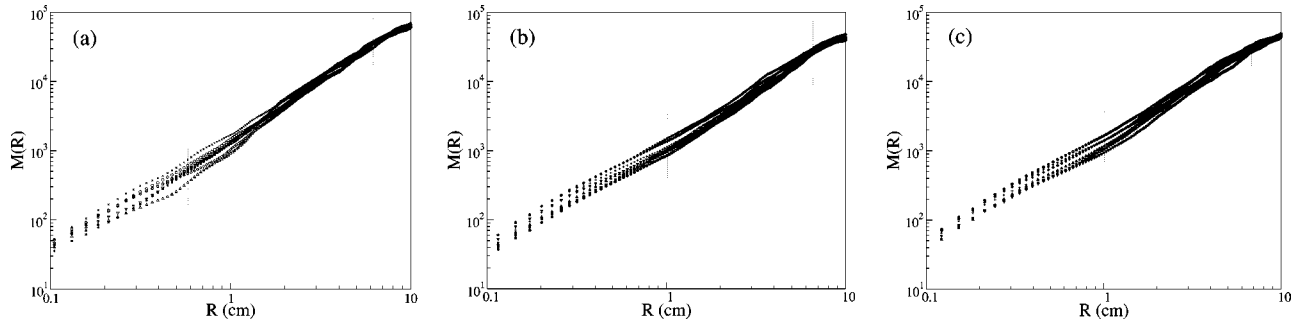


FIG. 3. Mass-size dependence for seven equivalent configurations of crumpled wires in the TP limit for (average) $p[L(\text{cm})]=0.139$ [438], 0.116 [363], and 0.135 [423]; respectively for $\theta=180^\circ$ (a), 90° (b), and 10° (c). The averaged mass in the scaling region (delimited by dotted lines in the figure) behaves as $M(R)\sim R^D$, with $D=1.9\pm 0.2$, for $\theta=180^\circ$, and $D=1.8\pm 0.2$, for $\theta=90^\circ$, and 10° . See Sec. III A for details.

of Figs. 3(a)–3(c) in arbitrary units, for TP configurations of 2D crumpled wires associated with 7 equivalent samples with *average* maximum packing fraction (length) given by $p[L(\text{cm})]=0.139$ [438], 0.116 [363], and 0.135 [423]; respectively, for $\theta=180^\circ$, 90° , and 10° . In the plots of Fig. 3 we can observe that the mass (or projected area) of the crumpled structures display a tendency to scale as a power law in R over two decades, from $R=0.1$ cm to $R=R_0=10$ cm. From these figures, we obtain $M(R)\sim R^D$, with $D(\theta=180^\circ)=1.9\pm 0.2$, and $D(\theta=90^\circ)=D(\theta=10^\circ)=1.8\pm 0.2$, within the scaling interval delimited by the dotted lines in Fig. 3. Our overall estimate is

$$M\sim R^D, D=1.9\pm 0.2, \quad (2)$$

in the TP limit for all injection geometry. Of course, the true mass-size exponent for the TP configurations in Eq. (2) could be the Euclidean exponent $D_E=2$.

The exponent D in Eq. (2) can be related to the distribution functions $n(s)$ or $n(l)$, giving the respective number of loops of internal area s or perimeter l , and to the energy E needed to form a loop of a certain size. To see this, first note that the work needed to form a TP configuration with a length L of wire injected into the cavity is simply $W=F_{ext}\times L$, where F_{ext} is the available (constant) average external force to perform the packing process. The work W can also be calculated as

$$W=\int_{l_{min}}^{l_{max}} n(l)E(l)dl=\int_{s_{min}}^{s_{max}} n(s)E(s)ds,$$

where $n(l)dl=n(s)ds$. If we use the simple scaling hypotheses for the TP limit: $s\sim l^2$ (to be confirmed in Sec. III F), $n(s)\sim s^{-\tau}$ (such a power law is in conformity with the cascade of loops mentioned in Sec. II; see also Sec. III E), and $E(s)\sim s^\alpha$, $\alpha>0$; with s_{min} dependent on the length scale ζ , and $s_{max}\sim R^2$, we obtain

$$W\sim M\sim R^D, D=2(1+\alpha-\tau). \quad (3)$$

From Eqs. (3) and (2) we conclude that $\alpha=\tau$ within typical statistical fluctuations of 10% in D . If we adopt a simple elastic energy quadratic in the linear size, i.e., with $E\sim l^2\sim s^\alpha$, $\alpha=1$, a distribution function for loops decaying as

$n(s)\sim s^{-1.0\pm 0.1}$ is expected. In fact, this scaling distribution for $n(s)$ is not significantly different from the experimental result $n(s)\sim s^{-1.4\pm 0.2}$ reported in Ref. [22], and discussed in Sec. III E. Before concluding this section, some additional information on the method used to obtain $M(R)$ in Fig. 3 is in order. The measurement of M as a function of R was made in two steps: for $4\text{ cm}<R<10\text{ cm}$, $M(R)$ was measured within a single circle with origin at the geometrical center of the cell; and for $0.1\text{ cm}<R<4.0\text{ cm}$, $M(R)$ was taken as the average mass within 5 or 6 equivalent disjoint circles whose centers were localized in different points of the wire taken at random but subject to the further constraint of nonoverlap with the border of the cell. This procedure is important to counterbalance an expected distortion leading to a depletion of the mass near the center of the cell if a single circle is used. The effect due to one-center sampling is illustrated in Fig. 4, which shows the same type of plot as that in Fig. 3(a), but with $M(R)$ measured only in circles whose centers coincide with the center of the cell. In order to give a better account of the mass-size dependence in these packing processes, we exhibit in Fig. 5 the mass-size relation for wires with $p[L(\text{cm})]=0.0477$ [150], for all types of injection studied. In these cases we obtain sensibly different effective exponents, namely, $D(\theta=180^\circ)=1.35\pm 0.10$, and $D(\theta=90^\circ)=D(\theta=10^\circ)=1.45\pm 0.10$. A possible guess regarding the nature of the configurations of crumpled wires in our experiments includes an analogy with the conformations of self-avoiding random walks or linear polymers [23]. Self-

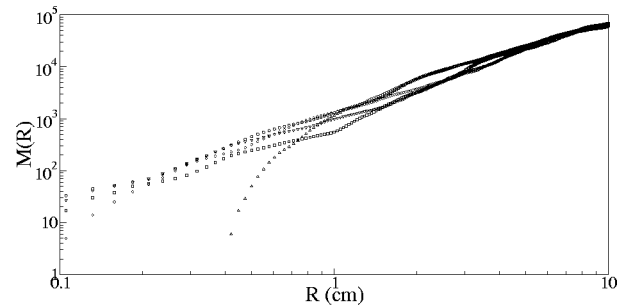


FIG. 4. The same mass-size relation for the crumpled wires as in Fig. 3(a) (TP limit, $\theta=180^\circ$), but using only circles with origin at the center of the cell: the quality of the scaling relation reduces. See Sec. III A for details.

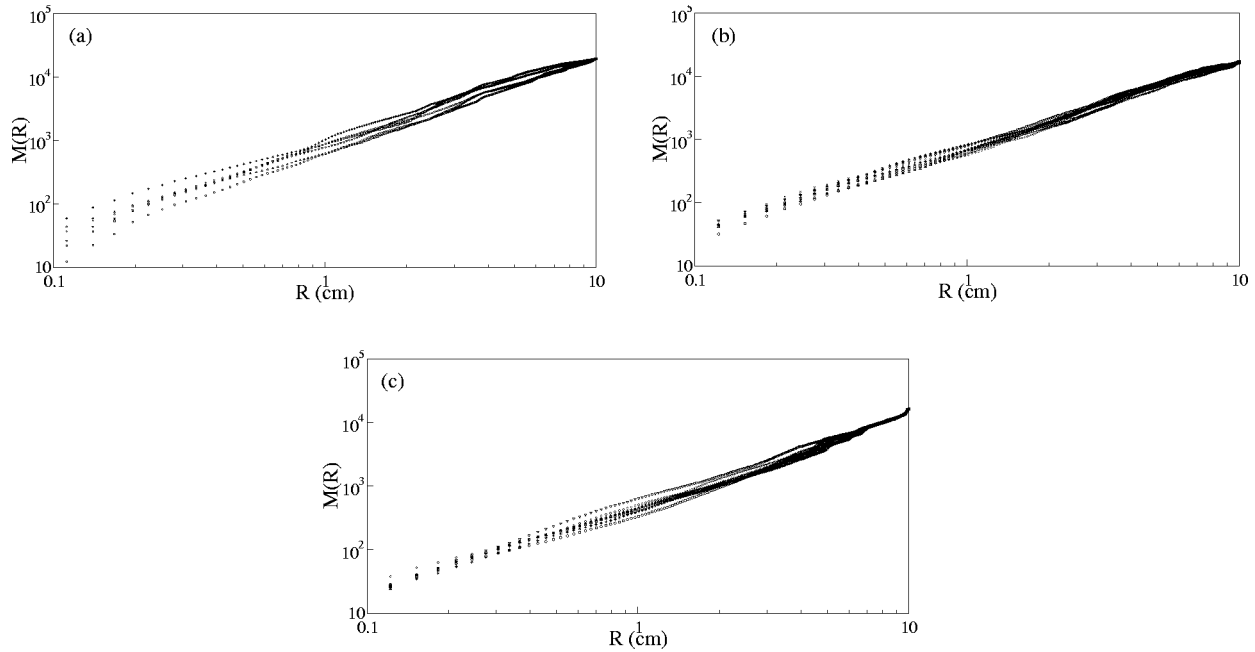


FIG. 5. Mass-size relation for wires with $p [L(\text{cm})]=0.0477[150]$, for all types of injection studied. In these cases we obtain sensibly different effective exponents (as compared with those of Fig. 3): $D_{eff}=1.35\pm 0.10$, for $\theta=180^\circ$ (a), and $D_{eff}=1.45\pm 0.10$, for $\theta=90^\circ$ (b) and 10° (c). These values are reminiscent of the Flory exponent $4/3$ for self-avoiding random walks in two dimensions. See Sec. III A for details.

avoiding random walks properly weights the conformations available to a real linear chain polymer [24]. Crumpled wires and real polymers are expected to be similar in some sense because both systems refer to unbranched flexible chains of matter submitted to elastic and excluded-volume interactions. The Flory analysis for this type of polymer predicts a mass-size exponent $D=4/3$ in two dimensions [23]. This last value is in close agreement with the numerical results of D_{eff} reported in Fig. 5, which is for crumpled wires associated with packing fractions greater than p_{fc} (1.4% to 2.3%) and less than p_{max} (13% to 15%).

B. Box counting for 2D crumpled wires

The geometric properties of the crumpled wires were additionally studied with the box-counting method [25] by counting the number $N(\epsilon)$ of squares of size ϵ needed to cover the crumpled structures. We exemplify in Fig. 6 the corresponding log-log plot of the (averaged) $N(\epsilon)$ versus ϵ associated with the structures studied in Fig. 3(a), that is, for the TP limit, and $\theta=180^\circ$. The plot in Fig. 6 shows that $N(\epsilon)$ scales as $\epsilon^{-D'}$, where D' is the fractal dimension of the 2D crumpled wire. The exponent D' has the values 1.8 ± 0.2 ; i.e., D' is the same as the mass-size exponent D within the statistical fluctuations. The mass-size exponent D is equal to the exponent D' obtained from the box counting (within statistical fluctuations of 10%) also for the geometries with $\theta=90^\circ$ and 10° .

C. Number of loops

As the packing fraction of the wire injected into the cavity increases, the total number of loops n_l formed as a conse-

quence of wire-wire contacts also grows. The experimental dependence of n_l with p (averaged on seven equivalent experiments) (■) and the corresponding fluctuations are shown in Fig. 7. The log-log plot of $n_l(p)$ shows two different behaviors: a shoulder for $p\leq 0.032$ and a power-law asymptotic dependence $n_l\sim p^{1.6\pm 0.2}$, for $0.032\leq p\leq 0.140$. The rate of loop formation presents the largest value in the beginning of the first region, when the incipient CW behaves as a soft structure. The number of loops n_l is needed to calculate the average coordination number in the following section.

D. Number of contacts wire-wire and number of coordination

Two important statistical quantities are the number of wire-wire contacts n_{ww} as a function of p , as well as the

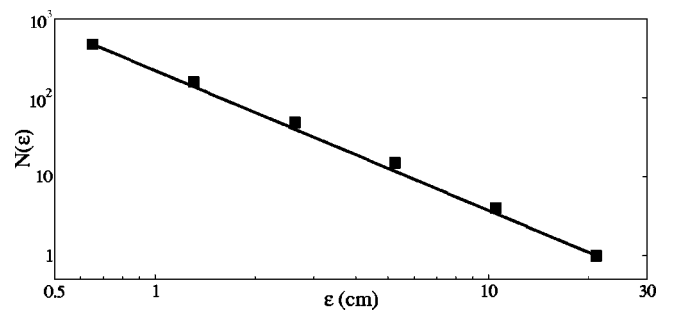


FIG. 6. Log-log plot of the (average) number $N(\epsilon)$ of boxes of size ϵ needed to cover each one of the seven equivalent configurations of 2D crumpled wire associated to Fig. 3(a) (TP limit, $\theta=180^\circ$) as a function of ϵ . The scaling exponent $D'=1.8\pm 0.2$ in $N(\epsilon)\sim\epsilon^{-D'}$ agrees with the mass-size exponent D of Fig. 3(a). See Sec. III B for details.

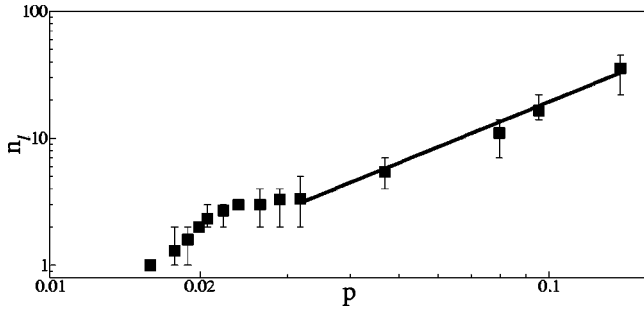


FIG. 7. The dependence of the number of loops n_l with the packing fraction p , averaged on seven equivalent experiments (■), and the corresponding fluctuations.

averaged number of different loops which are in contact with a single loop or, simply, the average coordination number γ ; both are particular cases of the kissing number problem [5]. In Fig. 8 we exhibit n_{ww} as a function of p ; n_{ww} is greater than the number of contacts loop-loop n_{ll} presented in Ref. [22], because now we need to add to n_{ll} the number of contacts to form all the loops ($=[1 \text{ contact per loop}] \times [n_l \text{ loops}] = n_l$ contacts) and the number of contacts of a loop with a nonloop. As shown in Fig. 8, n_{ww} scales as $n_{ww} \sim p^{2.0 \pm 0.1}$ along one decade, with small statistical fluctuations. This experimental result is reminiscent of Flory's mean field argument, which suggests that n_{ww} should scale with the density of repulsive energy within a particular configuration of crumpled wire, that is with p^2 [23]. The average coordination or kissing number $\gamma = n_{ll}/n_l$, is an important statistical parameter in disordered packings: in our experiment, γ increases asymptotically as $\gamma \sim p^{0.7 \pm 0.2}$. This last exponent must be considered with a grain of salt because it is deduced using the short interval $0.045 \leq p \leq 0.140$, as shown in the inset of Fig. 8. It can be noticed from this inset that $\gamma \approx 1.5$ at the TP limit; this value is less than half the mean

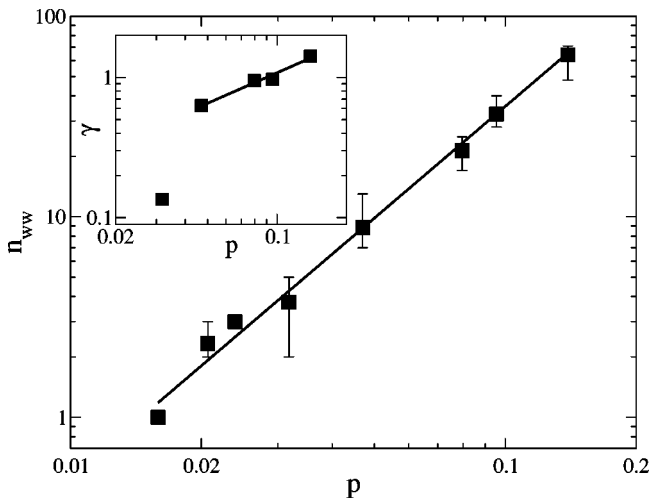


FIG. 8. The average total number of contacts wire-wire n_{ww} scales as $n_{ww} \sim p^{2.0 \pm 0.1}$ along one decade. The inset shows the average coordination or kissing number γ , which increases asymptotically as $\gamma \sim p^{0.7 \pm 0.2}$, in the interval $0.045 \leq p \leq 0.140$. See Sec. III D for details.

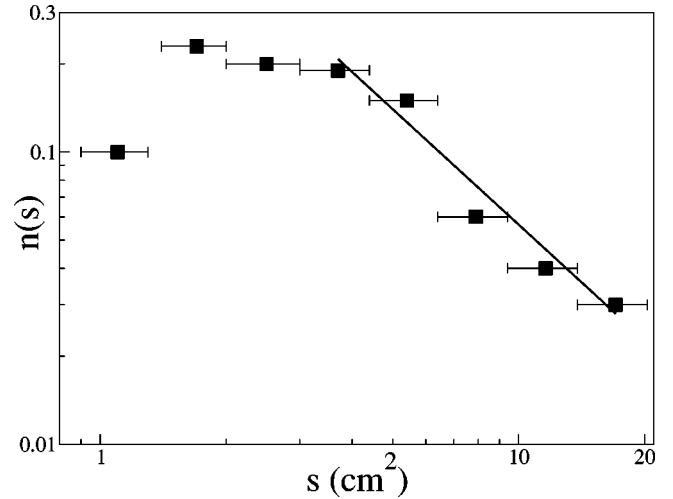


FIG. 9. Distribution function $n(s)$ for loops with area s in the TP limit. The straight line represents the adjust $n(s) \sim s^{-1.4 \pm 0.2}$. See Sec. III E for details.

contact coordination found in many 2D packing of discs with size distribution studied by Bideau and Troadec [11]. Moreover, the value $\gamma \approx 1.5$ for crumpled wire in the TP limit is very close to the number of coordination found in some 2D disordered packings, namely, the face-to-face coordination number for regular polygons of 9 faces ($\gamma_{ff}^9 = 1.34$), and the vertex-to-face coordination number for packing of regular triangles ($\gamma_{vf}^3 = 1.73$) [13].

E. Distribution function for areas of loops

We observe that the TP limit in our experiment is associated with 2D configurations of crumpled wires with a total number of loops varying in the interval $n_l = 22$ to $n_l = 45$, with an average $\langle n_l \rangle \approx 35.5$. In all we had 249 loops for seven equivalent experiments of crumpled wires with the largest packing fractions. If these loops are divided in bins according their respective areas s , we obtain the distribution function $n(s)$ which is shown in Fig. 9. The linear fit in this figure gives an asymptotic power-law behavior over about a decade: $n(s) \sim s^{-\tau}$, with $\tau = 1.4 \pm 0.2$. The expected value for the exponent τ is $\tau = (D + d - 1)/d = 1.45 \pm 0.10$, in good agreement with the experimental data [22]. A cascade of loops satisfying a scaling distribution of sizes seems to optimize the occupation of space by a flexible wire. For many-loop structures distant from the TP limit, the total number of loops is smaller, and $n(s)$ does not scale as a power law.

F. Perimeter-area relation for loops

For 2D Euclidean figures of any shape we know that the relation between perimeter P and area delimited by the perimeter, s , obeys the scaling $P = k s^{1/2}$, with k dependent on the particular shape of the figure. In order to quantify the geometry of the loops in our experiment, we evaluate both perimeter and area for each loop within the range $20 < s(\text{mm}^2) < 2000$ in seven equivalent experiments in the TP limit. This interval of s assures the 2D character of the packing: the smallest loops in this interval have a typical length

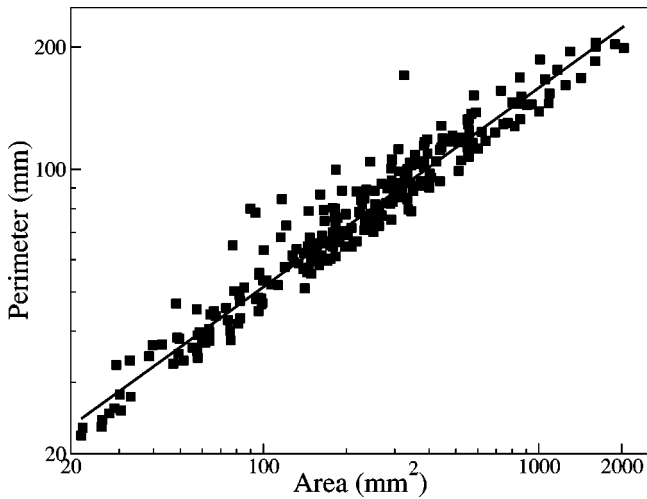


FIG. 10. Perimeter (P)-area (s) relation for loops in the TP limit. The continuous line in this figure represents the best fit $P(\text{mm}) = (5.8 \pm 2.1)s^{0.49 \pm 0.07}$ along two decades in s , for $\theta = 180^\circ$. See Sec. III F for details.

considerably larger than the height of the cavity. The dependence between these two variables is exhibited in the log-log plot of Fig. 10 along two decades of variability in s . Figure 10 indicates that the shape of the loops is a statistically invariant property of the loops at least in the two-decade interval of area considered. The continuous line in this figure represents the best fit $P = (5.8 \pm 2.1)s^{0.49 \pm 0.07}$ for $\theta = 180^\circ$, where P and s are given in mm and mm^2 , respectively. It is interesting to notice that the value $k = 5.38$ is significantly greater than $k = 2\pi^{1/2} \cong 3.544 \dots$ for circles, and significantly greater than the largest value observed for regular polygons: $k = 2 \times 3^{3/4} \cong 4.559 \dots$, for equilateral triangles. For $\theta = 90^\circ$ and 10° we obtain, respectively, $P = 5.14 s^{0.50}$ and $P = 4.93 s^{0.50}$.

IV. CRUMPLED WIRE, DISORDERED FOAM, AND PACKING OF DISKS

As we have commented in the end of Sec. II, the mechanical behavior of the samples of crumpled wires is quite different near and well below the maximum packing fraction p_{max} . For $p \ll p_{max}$, the structures of wire examined in this work are soft, and it is relatively easy to introduce wire into the cavity; for $p \lesssim p_{max}$, the rigidity increases rapidly and the difficulty to insert more wire increases in the same way. Based on our experimental results, we estimate that for $p = p_{max} = 0.14 \pm 0.02$, for any of the three modes of injection examined, the crumpled structure is so rigid, that the wire becomes completely jammed within the cavity, being nearly impossible to continue its injection.

The crumpled wires we are dealing with and disordered 2D foam have a formal similarity in the sense that both are disordered 2D cellular structures composed of two different phases: a condensed-phase (metal in the crumpled wire case, and liquid in the foam case), and a less-condensed phase (basically air in both cases). In crumpled wires the mass is concentrated on the wires, while in froth the mass of liquid is concentrated in Plateau borders and borders junction [26].

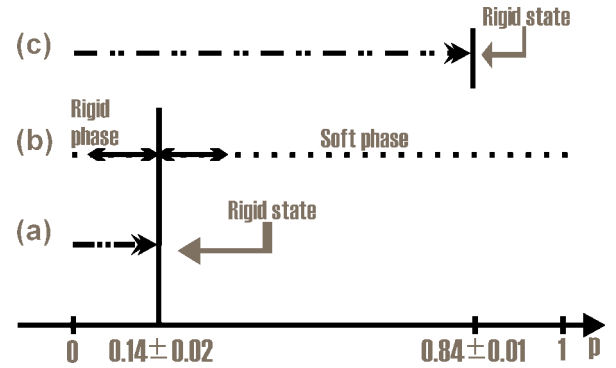


FIG. 11. Schematic representation of the soft and rigid domains observed in the three classes of disordered 2D structures discussed in Sec. IV: (a) crumpled wire ($p > 0.14 \pm 0.02$ is inaccessible), (b) soap foam, and (c) packing of disks ($p > 0.84 \pm 0.01$ is inaccessible).

Computer simulation shows that 2D disordered soap foam undergoes a transition *rigid* \rightarrow *soft* when the condensed-phase (liquid) reaches a packing fraction $p_{cp} = 0.16$ from below or, equivalently, when the packing fraction of the less-condensed-phase (air) reaches the value $1 - 0.16 = 0.84$ from above [27]. If $p > 0.16$, the shear modulus of the foam goes to zero, because the Plateau borders formed by liquid percolate and the system is now formed by isolated (circular) bubbles. Boltom and Weaire [27] argued that this value p_{cp} is associated with the problem of random close packing of disks in 2D. In fact, Bideau and Troadec have shown that there is a wide range of random mixtures of hard disks (i.e., the condensed phase in the packing of disks) for which the packing fraction is 0.84 ± 0.01 , independently of the relative concentration and size of the disks [11]. In 2D foam, the limit $p_{cp} = 0.16$ for the condensed phase is complementary to 0.84 obtained for disks. We conjecture that 2D crumpled wires undergo for *any* mode of injection of the wire in the cavity, i.e., not only for the three modes of injection studied in this work, a transition *soft* \rightarrow *rigid* when the packing fraction p associated with the wire approaches $p_{max} = 0.14 \pm 0.02$. This concentration is equal to p_{cp} for foams within the statistical fluctuations, and complementary to 0.84 ± 0.01 for random mixtures of hard disks. Thus, if $p < 0.14 \pm 0.02$, we can always introduce wire in the cell without much difficulty, but as long as the solid fraction p approaches the critical limit 0.14 ± 0.02 , the crumpled wire rapidly reaches a jammed (rigid) state. Our experiments suggest that this critical limit is robust, and valid *irrespective* of the mode of injection of wire, and the state of lubrication or dryness of the cavity. For $p > p_{max}$, further injection of wire is impossible for all practical purposes. The conjectured relationship among 2D crumpled wire, 2D disordered soap foam, and 2D random packing of disks is summarized in Fig. 11: (i) Random packing of disks with size distribution (top horizontal line) can attain a maximum packing fraction of 0.84 ± 0.01 ; (ii) disordered soap foam (intermediate line) can be observed with packing fraction of the liquid phase (p) in the entire interval $0 \leq p \leq 1$. However, foam undergoes a transition from a rigid phase to a soft phase, when p crosses the value 0.16 from below, and undergoes a transition from a soft

phase to a rigid phase, when the same line is crossed in the reverse direction. In particular, $p=0$ means a perfectly dry foam, whereas $p=1$ represents the uniform liquid state. (iii) Crumpled wire can attain (obviously only from below, as hard disks) a maximum packing fraction of 0.14 ± 0.02 , irrespective of the mode of injection and the state of lubrication of the cavity.

V. SUMMARY AND CONCLUSION

We have studied experimentally in detail the geometry of packings of crumpled wires in a two-dimensional cavity and, in particular, the dependence of several statistical properties of such structures with the packing fraction p of the wire. Many scaling laws connecting variables of interest are reported in Sec. III, and the associated critical exponents are found to be independent of the form of injection of the wire in the cavity. It is shown that there are *soft* and *rigid* domains of behavior for crumpled wires, dependent upon the packing

fraction. We conjecture that crumpled wires in 2D attain a rigid state, as observed for random packing of disks and disordered 2D soap foam [27], when the packing density of wire approaches the value 0.14 ± 0.02 , irrespective of the mode of injection and the state of lubrication of the cavity. This surprisingly low packing fraction is complementary to that observed in the 2D disordered packing of disks within the statistical fluctuations.

ACKNOWLEDGMENTS

The authors acknowledge stimulating discussions with G. L. Vasconcelos, L. C. de Mélo, J. R. Rios Leite, and O. N. Mesquita. This work was supported in part by Conselho Nacional de Desenvolvimento Científico e Tecnológico, Financiadora de Estudos e Projetos, Fundo Setorial do Petróleo, and Programa de Núcleos de Excelência (Brazilian Agencies).

-
- [1] *Disordered and Granular Media*, edited by D. Bideau and A. Hansen (North-Holland, Amsterdam, 1993).
 - [2] S. Jasty, M. Al-Naghy, and M. de Llano, *Phys. Rev. A* **35**, 1376 (1987); R. Radhakrishnan, K.E. Gubbins, and M. Sliwinski-Bartkowiak, *Phys. Rev. Lett.* **89**, 076101 (2002).
 - [3] S. Torquato, T.M. Truskett, and P.G. Debenedetti, *Phys. Rev. Lett.* **84**, 2064 (2000).
 - [4] O. Pouliquen, M. Nicolas, and P.D. Weidman, *Phys. Rev. Lett.* **79**, 3640 (1997).
 - [5] J.H. Conway, and N.J.A. Sloane, *Sphere Packings, Lattices and Groups* (Springer, New York, 1988).
 - [6] J.D. Sherwood, *J. Phys. A* **30**, L839 (1997).
 - [7] J.G. Parkhouse and A. Kelly, *Proc. R. Soc. London, Ser. A* **451**, 737 (1995); A.P. Philipse, *Langmuir* **12**, 1127 (1996).
 - [8] D. Coelho, J.-F. Thovert, and P.M. Adler, *Phys. Rev. E* **55**, 1959 (1997).
 - [9] M.A.F. Gomes and V.M. Oliveira, *Philos. Mag. Lett.* **78**, 325 (1998).
 - [10] H.T. Croft, K.J. Falconer, and R.K. Guy, *Unsolved Problems in Geometry* (Springer, New York, 1991).
 - [11] D. Bideau and J.P. Troadec, *J. Phys. C* **17**, L371 (1984).
 - [12] B.J. Brosilow, R.M. Ziff, and R.D. Vigil, *Phys. Rev. A* **43**, 631 (1991).
 - [13] M. Ammi, D. Bideau, and J.P. Troadec, *J. Phys. D: Appl. Phys.* **20**, 424 (1987).
 - [14] P.A. Houle and J.P. Sethna, *Phys. Rev. E* **54**, 278 (1996).
 - [15] A.E. Lobkovsky, S. Gentges, H. Li, D. Morse, and T.A. Witten, *Science* **270**, 1482 (1995); A.E. Lobkovsky, *Phys. Rev. E* **53**, 3750 (1996); M. Ben Amar and Y. Pomeau, *Proc. R. Soc. London, A* **453**, 729 (1997); E. Cerda and L. Mahadevan, *Phys. Rev. Lett.* **80**, 2358 (1998); B.A. DiDonna, T.A. Witten, S.C. Venkataramani, and E.M. Kramer, *Phys. Rev. E* **65**, 016603 (2001).
 - [16] J.-M. Debievre and R.M. Bradley, *J. Phys. A: Math. Gen.* **22**, L213 (1989).
 - [17] Y. Kantor, M. Kardar, and D.R. Nelson, *Phys. Rev. Lett.* **57**, 791 (1986); M. Plischke and D. Boal, *Phys. Rev. A* **38**, 4943 (1998); A. Baumgärtner, *J. Phys. I* **1**, 1549 (1991); F.F. Abraham and M. Kardar, *Science* **252**, 419 (1991); X. Wen, C.W. Garland, T. Hwa, M. Kardar, E. Kokufuta, Y. Li, M. Orkisz, and T. Tanaka, *Nature (London)* **355**, 426 (1992); E. Bouchaud and J.-P. Bouchaud, *J. Phys. (France)* **50**, 829 (1989).
 - [18] E.M. Kramer and A.E. Lobkovsky, *Phys. Rev. E* **53**, 1465 (1996).
 - [19] J.A. Aguiar, M.A.F. Gomes, and A.S. Neto, *J. Phys. A: Math. Gen.* **24**, L109 (1991); M.A.F. Gomes, F.F. Lima, and V.M. Oliveira, *Phil. Mag. Lett.* **64**, 361 (1991); J.B.C. Garcia, M.A.F. Gomes, T.I. Jyh, and T.I. Ren, *J. Phys. A* **25**, L353 (1992); M.A.F. Gomes and G.S.V. Melo, *Philos. Mag. Lett.* **68**, 191 (1993).
 - [20] H. Lodish, A. Berk, S. L. Zipursky, P. Matsudaira, D. Baltimore, and J. Darnell, *Molecular Cell Biology* (Freeman, New York, 2000).
 - [21] A. Maritan, C. Micheletti, A. Trovato, and L.R. Banavar, *Nature (London)* **406**, 287 (2000).
 - [22] C.C. Donato, M.A.F. Gomes, and R.E. de Souza, *Phys. Rev. E* **66**, 015102(R) (2002).
 - [23] P.-G. de Gennes, *Scaling Concepts in Polymer Physics* (Cornell University Press, Ithaca, 1985).
 - [24] J. Rudnick and G. Gaspari, *Science* **237**, 384 (1987).
 - [25] B.B. Mandelbrot, *The Fractal Geometry of Nature* (Freeman, New York, 1983).
 - [26] D. Weaire and S. Hutzler, *The Physics of Foams* (Clarendon Press, Oxford, 1999).
 - [27] F. Bolton and D. Weaire, *Phys. Rev. Lett.* **65**, 3449 (1990).